Methodology of Cell Selection and Modeling of Cell Performance for Aerospace Application

An Undergraduate Honors Thesis

Submitted to the Department of Electrical and Computer Engineering

The Ohio State University

In Partial Fulfillment of the Requirements for Graduation with Honors Research Distinction in Electrical Engineering

David Wolfson

Spring, 2019

Dr. Marcello Canova, Advisor

Abstract

The electric vehicle industry has more than 20 years of experience in designing battery packs for automotive and small UAV (unmanned aerial vehicle) application. These battery packs consist of a combination of cells that are wired together in series and parallel to achieve the proper voltage and power/energy requirements for that vehicle. In general, the packs are designed to work at standard operating conditions of temperature (-30 – 60°C) and pressure (atmospheric).

The aerospace industry is recently considering the on-board integration of energy storage elements (batteries) to improve fuel burn and carbon dioxide emission. The industry is looking at mainly a hybrid propulsion system, integrating the energy storage elements with the traditional turboshafts and generators. However, a battery back for aerospace application must be designed for use in temperatures reaching -60°C, a pack voltage of up to 2000 volts, and approximately 8 megawatts of power.

One major obstacle that arises when creating a battery pack of this size and capability is that testing and building prototype battery packs is extremely inefficient regarding both cost and time. In order to bypass this obstacle, models are created to simulate the behavior of the battery pack. This research project will focus on the methodology of experimental testing methods to select the most fitting cell technology for aerospace application and the development of numerical models to characterize the cell's behavior for a given power schedule the pack will be subject to during flight. Multiple tests are needed to be run on the battery cells, including Multi-Rate Capacity tests, HPPC (Hybrid Pulse Power Characterization) tests. The data from these tests needs to be analyzed to select which technology is most fitting, then a model needs to be created that characterizes the cell's characteristics and simulates how the battery pack will perform during flight.

Acknowledgements

I would like to thank Dr. Marcello Canova for advising me on this research project. His expertise in batteries and cell modelling were integral to this project. Dr. Canova helped guide me through the entire research process and the achievement of my honor's thesis. The advice that he gave me was crucial to the successful completion of this project.

I would also like to thank Dr. Yann Guezennec for his guidance in the battery testing and modelling process. His advice on equivalent circuit modeling appreciated and necessary for this project.

Additionally, I would like to thank Matilde D'Arpino and Prashanth Ramesh for their help throughout the entire research project. Their guidance on how to approach and conduct data analysis and model development was indispensable and critical to the completion of this thesis.

Table of Contents

List of Figures and Tables:

Chapter 1: Introduction and Background

The aviation industry has been growing tremendously over the past two decades due to an increase in the number of passengers and the growth of ecommerce. This growth of the industry results in higher aviation traffic and therefore significantly higher fuel consumption [1], as currently all commercial aircrafts use gas turbine engines. To combat this dramatic increase in fuel consumption, the aviation industry has been conducting research into integrating electrification technology into aircraft.

The Ohio State University (OSU), in collaboration with NASA and other universities as part of a University Leadership Initiative (ULI) project, is leading the effort in evaluating challenges and opportunities in the design of hybrid electric aircrafts for short range transportation [2]. This program plans to design components and systems to enable the electric aircraft of the future, focusing on energy storage systems, distributed energy propulsion, high efficiency, safety, and reliability. The challenges that the project faces for integrating the Energy Storage Systems (ESS) into the aircraft is that the ESS is bulky, expensive and generates excess heat. The fuel used in a gas turbine engine is also more energy dense than an ESS. My contribution to this project is aiding in the cell selection process, developing models to characterize cell performance, and assisting in the battery pack design, all of which will be discussed further in Chapters 3 and 4.

1.1 Hybrid Electric Aircraft

The main focus of the NASA ULI is to design a Hybrid Electric Aircraft (HEA). Hybrid electric propulsion allows a vehicle to incorporate propulsion energy from two or more kinds of energy storage systems, sources, or converters, one of which must be electrical in nature [3].

When discussing the integration of hybrid electric technology into aircraft, there are three main architecture designs for the propulsion system of a HEA: parallel hybrid, turboelectric, and series/parallel hybrid [4]. The figure below shows the differences between these three powertrain architectures.

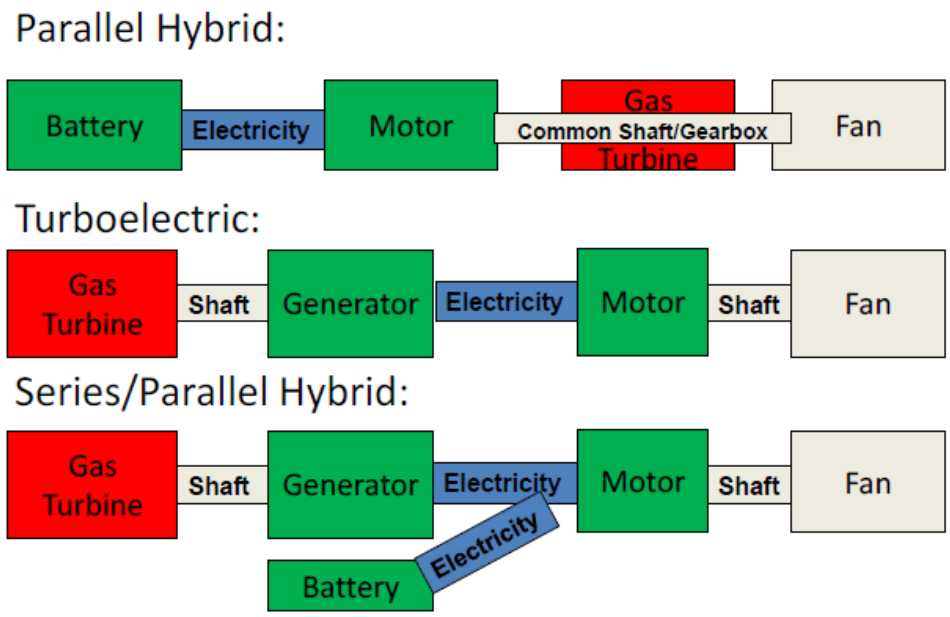

Figure 1: Powertrain Architectures [4]

A parallel hybrid is an architecture that powers a vehicle from both an energy storage element (usually a battery) and a conventional fuel engine. In the case of the hybrid electric aircraft, the fans are being mechanically driven by the gas turbine and the electric motors. This is typically done by using common shafts or gearboxes. It is important to note that there is no conversion of the mechanical energy to electric energy done before powering the fans.

Unlike the parallel hybrid, the turboelectric uses a gas turbine to produce the electric power that drive the fans. In this design, there are no energy storage elements. Rather, the mechanical energy produced from the gas turbine is converted to electric energy by the

generator, which then powers the motors to turn the fans. This architecture is not classified as hybrid since it does not integrate a battery storage element.

The series/parallel hybrid is the architecture that combines the parallel hybrid and turboelectric designs. A gas turbine produces mechanical energy that is converted to electric energy using the generator. An energy storage element (e.g. a battery) is also integrated as another source of electric energy for the motor. A battery pack can be recharged between flights on the ground or during flight by the gas turbine.

1.2 Benefits of Hybridization

Each architecture type for hybrid electric aircraft has its own advantages and disadvantages. As a whole, hybridization of any propulsion system, especially those of aircraft, offer several extremely important benefits, including fuel savings and reduced carbon dioxide and NOx emissions [5].

The integration of an energy storage element, like a battery, can dramatically reduce the fuel consumption of the aircraft. Instead of the power being completely sourced from the gas turbine, the ESS can provide additional power. Because it can now rely on the supplemented power provided by the battery for takeoff and climb, this turbine can be reduced in size accordingly. Moreover, a smaller turbine is more efficient than a turbine sized for normal aircraft operation. Therefore, the addition of the ESS into the aircraft reduces the fuel burn in two ways: less fuel is burned since the ESS supplements energy for takeoff and climb, and the turbine itself is more efficient, causing it to burn less fuel.

However, this concept of a smaller turbine is not applied to all hybrid electric aircraft. Some aircraft use standard turbines for operation that are supplemented by a battery pack. Even in this case, there is still a large amount of fuel savings, since the turbine is not the sole source of power for the aircraft.

With a reduction in fuel consumption, the amount of carbon dioxide and NOx that are produced by the gas turbine are proportionally reduced as well. Essentially, a gas turbine is combustion engine, so when the fuel is combusted, it produces carbon dioxide and NOx. Hence, reducing the amount of fuel burned will reduce the amount of these emissions.

1.3 Hybrid Electric Aircraft Concepts

In 2007, NASA set a goal of 20% reduction in fuel burn by aircraft entering service in 2015 – 2025 (compared to a 2005 baseline aircraft) [6]. In 2016, NASA has updated their goal of achieving this 70% fuel burn reduction to take place during the 2015-2025 period, as shown in Table 1. In response, many different companies and organizations have launched major research projects into the field of hybridizing aircraft.

Table 1:NASA's Goals for Future Aircraft [7]

Technology Benefits	Technology Generations (Technology Readiness Level = 5-6)		
	Near Term 2015-2025	Mid Term 2025-2035	Far Term Beyond 2035
Noise (cum below Stage 4)	22-32 dB	32-42 dB	42-52 dB
LTO NOx Emissions (below CAEP 6)	70-75%	80%	> 80%
Cruise NOx Emissions (rel. to 2005 best in class)	65-70%	80%	> 80%
Aircraft Fuel/Energy Consumption (rel. to 2005 best in class)	40-50%	50-60%	60-80%

In addition to NASA's own progress, companies such as Wright Electric, Boeing, and Rolls-Royce have all made significant progress in designing hybrid electric and turbo electric aircraft concepts. NASA has designed the NASA X-57 Maxwell, implementing a two-parallel battery pack consisting of 5120 Li-ion cells with a pack weight of 860 lbs. NASA has also designed STARC-ABL having a 3 MW power system. They predict this aircraft will have a 7-12% net fuel burn reduction [8]. Wright Electric aims to produce electric aircraft that are capable of flying short distances, no more than 300 miles. They have already built a two-seater proof-of-concept for UK budget carrier EasyJet, using a battery pack weighing 600 lbs [9].

Boeing has made considerable progress in their design of their HEA, called Boeing SUGAR Volt. SUGAR stands for Subsonic Ultra Green Aircraft Research. Different propulsion systems were explored during this project, including a fully battery-powered propulsion system and fuel cell/Brayton cycle hybrid propulsion system. Both of these designed were deemed unrealistic with the technology of the present-day. The propulsion system chosen is a battery/Brayton cycle hybrid propulsion system [4].

Rolls Royce designed an HEA called the eConcept Vehicle. The eConcept will utilize a series/parallel hybrid propulsion system. A single turbogenerator along with a large battery pack will power the aircraft's fans. During takeoff and climb, the battery pack will supply extra power, and during cruise, the batteries will be recharged by the turbogenerator. This differs from the SUGAR Volt, where the battery pack is charged on the ground between flights.

1.4 Challenges with Hybrid Electric Aircraft

Integrating batteries into commercial aircraft seems to be the solution to all the aforementioned problems with commercial aircraft today. In fact, batteries are being integrated in a type of aircraft called e-UAVs. Electric Unmanned Aerial Vehicles (e-UAVs) are powered completely by batteries. The battery packs are sized for short missions, which is the typical operation of a UAV. This allows the battery pack to be small and inexpensive. Additionally, since the vehicle is unmanned, there are fewer measures necessary to ensure safe operation of the e-UAV, and performance consistency of the pack is not a concern.

On the other hand, a regional aircraft operates with passengers aboard and often travel more than 100 miles in a single mission. Therefore, the battery pack of a regional HEA needs to be more consistent and reliable, safer, and significantly larger, causing it to be more expensive. Hence, the design and manufacturing of an HEA battery pack is more complex and expensive than that of e-UAVs.

The most important metrics when designing a battery pack are energy density (in Wh/kg) and power density (in W/kg). Currently, the state-of-the-art commercial battery technology has an energy density between 170 – 270 Wh/kg, as shown later in Figure 13 in Chapter 3. In order to develop a battery pack for a hybrid electric aircraft, the batteries must have an energy density of 400 – 500 Wh/kg. This type of battery technology is in the prototype stage, and it will be several years before the technology will become commercially available.

Furthermore, when compared to the typical combustion engine in an automobile, batteries are clearly lacking in performance. Energy density of gasoline for automobile application is about 47.5 MJ/kg while a Chevy Volt lithium-ion battery pack has an energy

density of only 0.3 MJ/kg [12]. Therefore, in certain cases, gasoline has approximately 150 times the energy density of a lithium-ion battery pack. Although fuel for aircraft is used less efficiently than in automobiles, jet fuel still produces about 43 times more energy than a battery of the same weight [13]. The Regone plot below in Figure 2 shows a comparison between different propulsion systems.

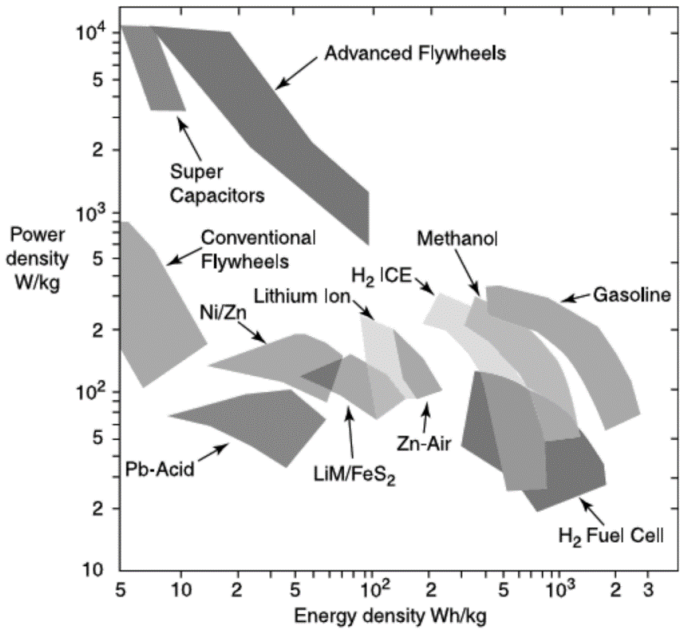

Figure 2: Regone Plot [14]

Although state-of-the-art cell technology does not current provide enough energy, the Department of Energy (DOE) has collected data suggesting that the power and energy of cells are increasing each year regardless of cell technology [15]. Figure 3 below shows the data trends collected by the DOE. If this trend continues, the possibility of building hybrid electric and fully electric aircraft will become a reality in the near future.

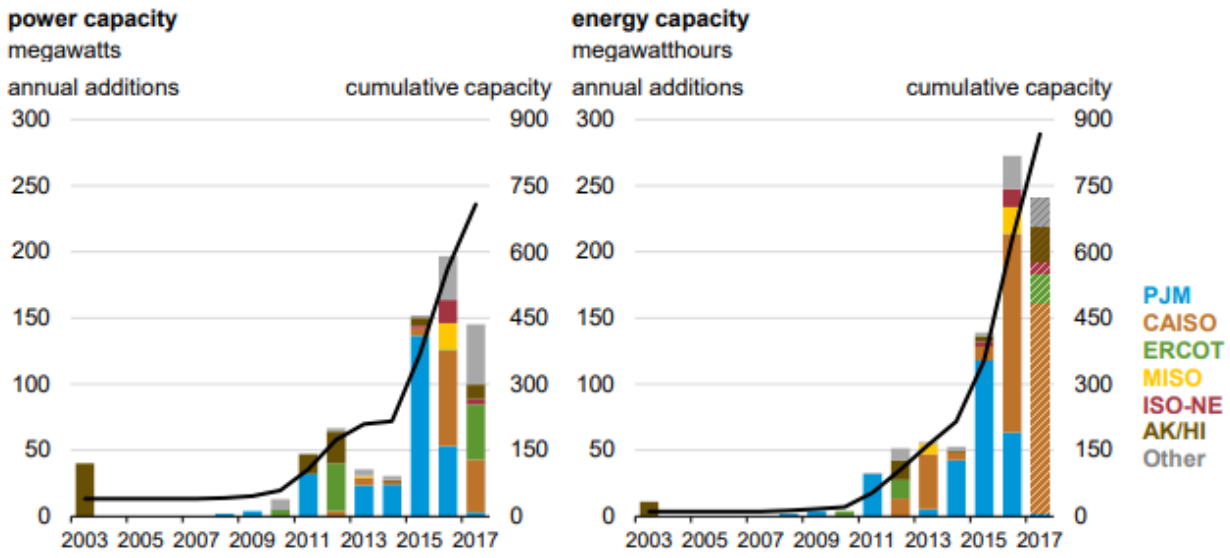

Figure 3: Power and energy trends

1.5 Thesis Overview and Contributions

This thesis will discuss general concepts regarding battery packs and their components, the methodology of cell selection for aerospace application, and the development of models used to simulate cell performance and aid in battery pack design. My contributions to the project were analyzing the data from tests conducted on the cells, investigating battery pack weight estimations, and 0^{th} and 1^{st} order model development and validation.

Chapter 2: The Battery Pack

Battery packs are made up of multiple different components all integrated together for the optimal performance of the pack. The pack is reliant on the integration and consistent performance of all components. If one of the components fails, the battery pack will not perform optimally.

2.1 Components

All electric vehicles battery packs consist of four main components; the battery cells and their packaging, the Battery Management System (BMS), the Thermal Management System (TMS), and the connectors/bus bars. Figure 4 below shows the layout of a generic battery pack for an electric vehicle. The battery pack for a hybrid electric vehicle consists of the same components and the same layout as the battery pack of an electric vehicle, with the addition of a gas turbine engine in the powertrain of the vehicle to supplement energy to the motor.

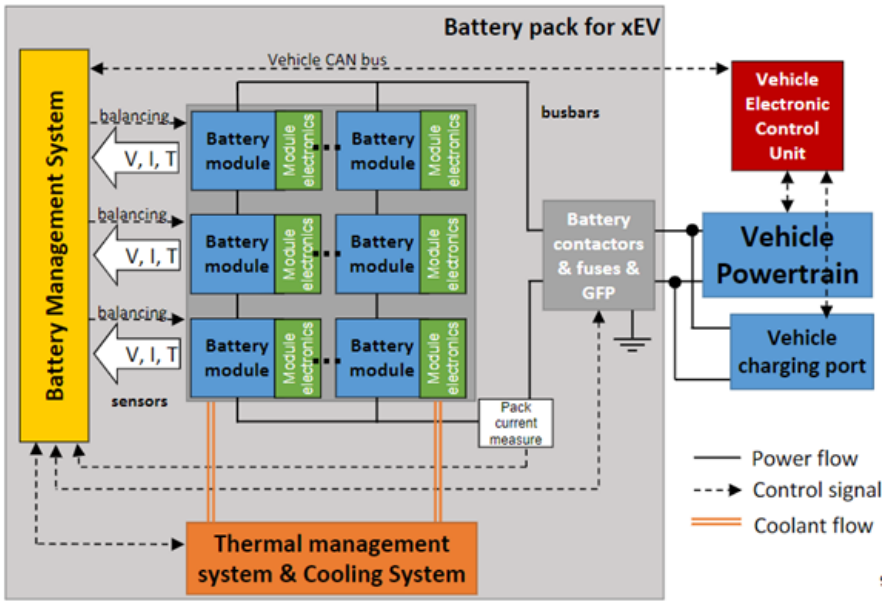

Figure 4: Electric vehicle battery pack layout

The battery pack itself is made up of hundreds, and sometimes thousands, of individual battery cells connected in series and parallel to achieve a specified energy and power. In order to correctly build the battery module and connect the cells in the optimal configuration, a target energy or power level needs to be specified. The cells in the modules are connected in series to achieve a specific voltage and power requirement, and these series chains are connected in parallel to achieve an energy requirement. Battery packs that need to achieve a high power tend to consist of a large number of cells being connected in series, with only two or three of these chains connected in parallel. The large number of cells in series causes the battery to have a large pack voltage, which leads to a high pack power. On the other hand, battery packs that need to achieve a high energy level tend to consist of a smaller number of cells connected in series but a larger number of these chains connected in parallel. Hence, battery packs are typically either energy battery packs or power battery packs. Figure 5 below shows the battery pack of a Tesla

Model S. Underneath the plastic cover lies hundreds of individual battery cells connected together to achieve an energy of 85 kWh and a pack voltage of 400 V_{DC} [16].

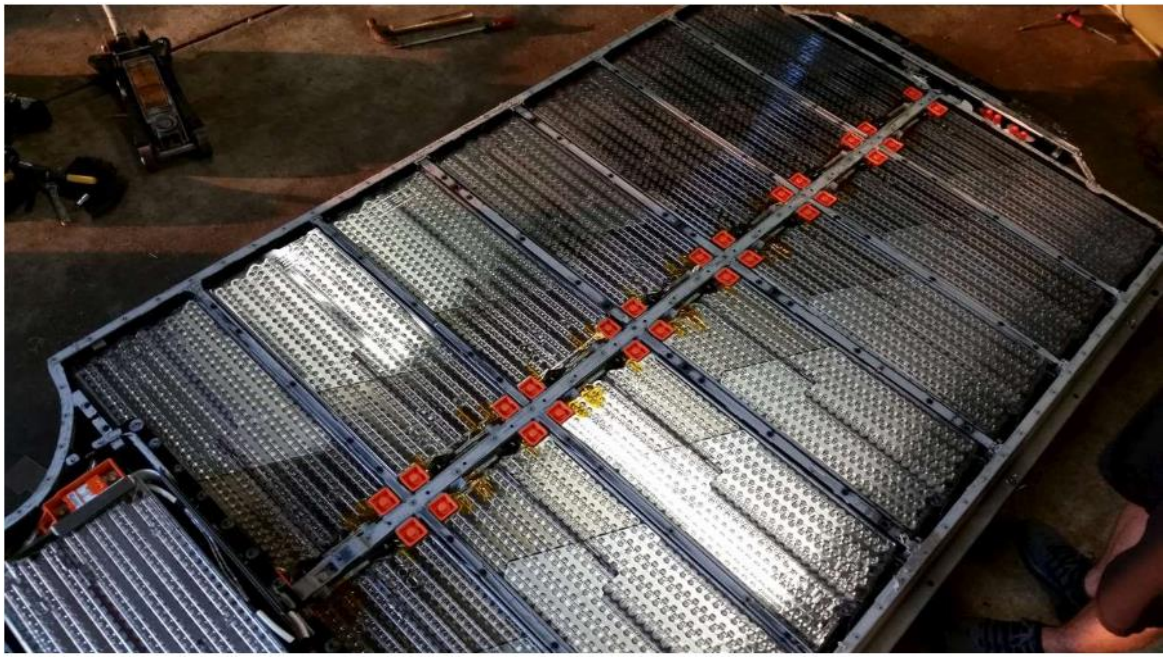

Figure 5: Tesla Model S battery pack [16]

As denoted in the previous paragraph, battery packs can be built up by connecting together smaller battery modules. The general practice in the electric vehicle industry is to create smaller battery modules that are connected in series and parallel to achieve an overall battery pack energy and power level. These battery modules are usually made up of between 10-100 individual cells. The reason for building modules (and not simply connecting all the cells together) is because if one of the cells in a series chain becomes unusable, that entire chain of 100+ cells connected in series becomes unusable and the entire chain needs to be replaced. Instead, with the modules, if one of the cells in the module becomes unusable, you can simply replace that faulty module, which is more time and cost efficient.

2.2 BMS and TMS

Along with the battery cells, two crucial parts to the optimal functionality of a battery pack are the Battery Management System (BMS) and the Thermal Management System (TMS). The battery management system is an electronic system used to protect and manage a rechargeable battery, such as a Li-ion cell. The BMS ensures that the cells do not operate outside of their safe operating range. For example, the voltage range of a NMC (Lithium Nickel Manganese Cobalt Oxide) cell is between 2.5 – 4.2 V. The BMS also controls the operating voltage of a chain of cells. For example, if one NMC cell in a chain of 50 cells in series is faulty in its operating range (the range is 2.7 – 3.9 V), that cell can cause problems in its chain. When the cells recharge, they will be recharged to the cells' maximum voltage, 4.2 V. This causes the faulty cell to be overcharged. Similarly, the chain will be discharged to the cells' minimum voltage, 2.5 V, causing the faulty cell to be over-discharged. The overcharging of a cell can cause the cell to go into thermal runaway, which will cause the entire series chain to go into thermal runaway. This can be extremely dangerous if not handled properly.

In order to combat this issue, the BMS forces all the cells in a series chain to operate in the voltage region of the weakest cell. Although this significantly reduces the performance of the chain, it ensures that the chain will not enter into thermal runaway. As an example (on a much smaller scale than what is considered in this study), a 25 amp-limit off-the-shelf battery management is shown below in Figure 6.

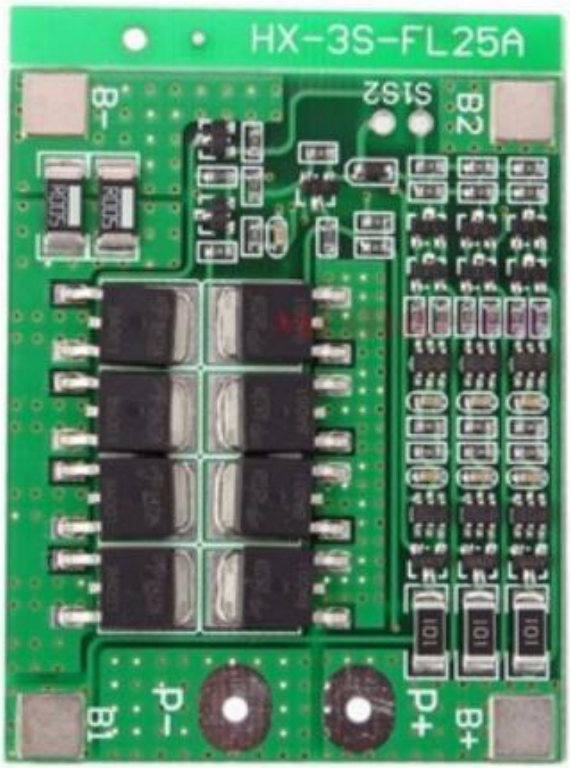

Figure 6: 25-amp limit BMS [17]

The thermal management system (TMS) is used to control the heat produced by the battery cells during discharge cycles. Especially when using Li-ion cells, large amounts of heat can be produced during discharge. Implementing a method to expel this heat is critical for maintaining capacity, life, and performance of the cell, and for ensuring the safe performance of the battery pack. The simplest method used in the industry is air-cooling, where the battery pack is exposed to the environment around it, allowing the pack to cool down by transferring heat to the environment or by forcing air cooling. Another common method used is a liquid-cooling system, where liquid is pushed through thin tubes that are wound in-between the cells, as shown in Figure 7. This allows the cells to transfer heat to the liquid. The liquid then dissipates that heat through radiators or another form of liquid-air heat dissipation.

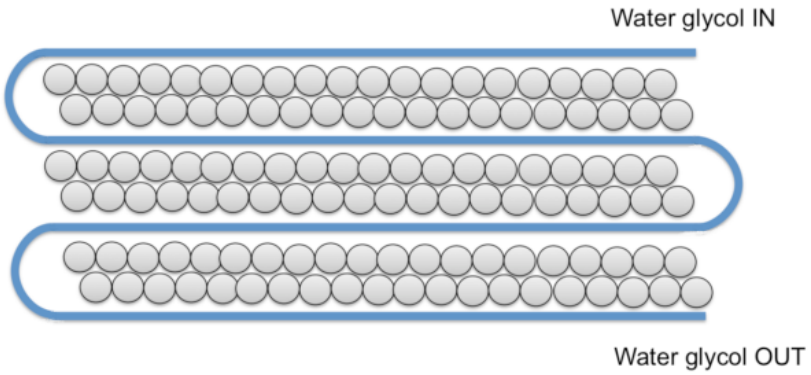

Figure 7: Liquid cooling TMS [18]

2.3 Battery Pack Design Process

A battery pack for automotive application needs to be designed considering electrical, thermal, and mechanical properties. The process begins by conducting multiple standardized tests on individual battery cells. The data from these tests are then analyzed and used to form a model of the cell that simulates performance for a given power schedule at the cell level. A power schedule is a profile of required output power by the cell over a certain period of time. The model is then validated to ensure it's within a given margin of error. Once the validation is complete, the model is scaled up from single cell to full battery pack to simulate battery pack performance.

The process begins with testing several different battery chemistries chosen. The cells then undergo Multi-Rate Capacity tests and Hybrid Pulse Power Characterization (HPPC) tests. These tests are generally conducted at room temperature and pressure, although they can be done at different temperatures and pressures depending on the application. There are several other tests that can be conducted as well, but the two previously-mentioned tests are the most widely used.

The Multi-Rate Capacity test and the HPPC test are used to show different aspects of the cell technology being tested. The Multi-Rate Capacity test is used to show how the capacity of

the cell changes when the cell is discharged at different current rates. The test consists of discharging the cell at different current rates and measuring the capacity of the cell. The general trend is that a cell's capacity degrades when discharged at higher currents. The better the technology, the smaller the loss of capacity in the cell when discharged at high current rates.

The data from Multi-Rate Capacity tests are used to determine whether or not a cell technology is viable for a certain application. Analysis of the data can show the decrease of the capacity with increased discharge current rates, as seen in Figure 8 below. In this figure (and throughout this thesis), currents are normalized as C-rates, where 1C is a current equal to the cell's capacity in Ah. If the cell's capacity decreases heavily at higher discharge current rates, then that cell is not fitting for an application that requires high capacity and high current discharge.

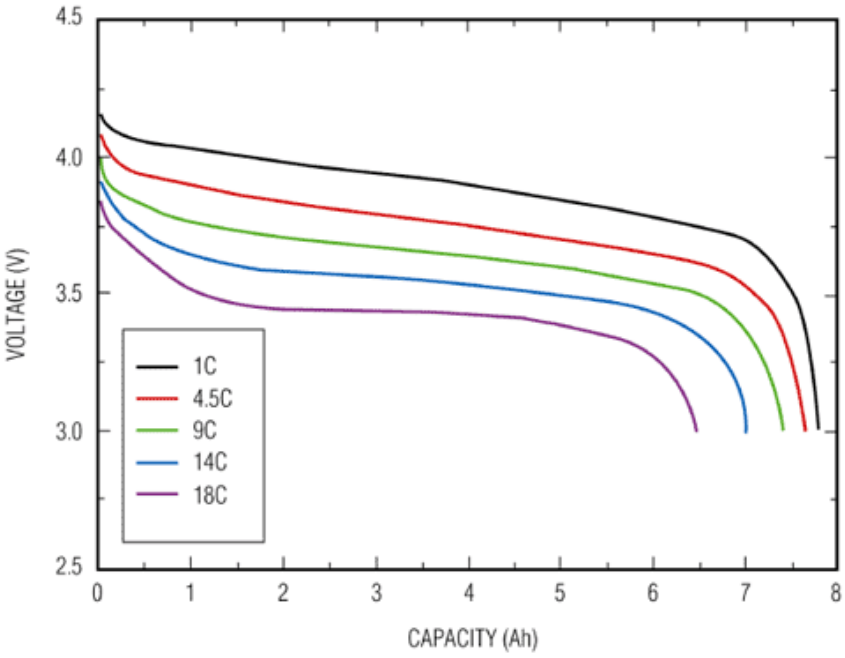

Figure 8: Multi-Rate Capacity test results [19]

The HPPC test uses precise discharging and charging of the cell to obtain several parameters, including internal resistance, open-circuit voltage (OCV), and the heat generated by

the cell. These parameters are then used to develop a model that characterizes the cell's performance. The parameters are typically calculated with respect to the state-of-charge (SOC) of the cell. The SOC is the amount of capacity left in the cell compared to the total capacity of the cell. State of charge is typically a percentage, and can be calculated using several different methods, the most popular method being Coulomb counting.

There are two categories of models used in literature to describe the behavior of battery cells – physic-based models (ex. electrochemical model) and empirical models (ex. equivalent circuit models). This thesis will discuss mainly the equivalent circuit model. The equivalent circuit model created from the HPPC data can have different orders depending on the needs of the application. A 0^{th} order model represents the cell as an ideal voltage source, approximated by the open circuit voltage (OCV) of the battery, and a single resistor in series, represented by the internal resistance. Figure 9 below shows the layout of a 0^{th} order model. Both the OCV (V_{OC}) and the internal resistance (R_0) will be calculated during the data analysis. The heat generation is calculated using the internal resistance and the discharge current. This model provides a reasonable approximation of a cell's performance.

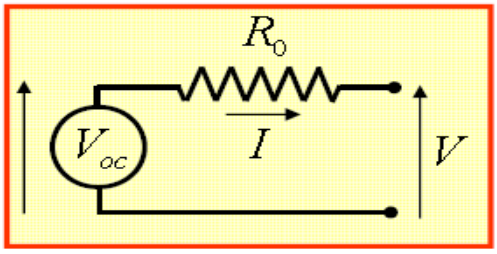

Figure 9: 0th order model

A more sophisticated model is a 1^{st} order model. A 1^{st} order model more accurately models the charge and discharge characteristics of a cell. The 1^{st} order uses an ideal voltage source (OCV) and series resistance, similar to the 0^{th} order model; however, this model

incorporates an RC block in series with R_0, as shown in Figure 10 below. This RC block is used to model the capacitor-like charge and discharge of a cell. These cell dynamics are ignored by the 0th order model, which assumes linear charge and discharge. For this reason, the 1st order model more accurately models the cell's performance than the 0th order model. However, the 1st order model is slightly more complicated and time-consuming to calibrate, which is why it is only used if the application requires a more accurate representation of the cell's dynamic effects.

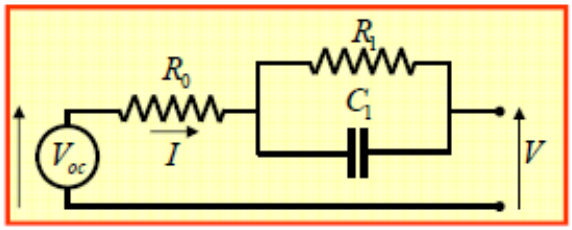

Figure 10: 1st order model

The cell model is developed and calibrated based on a single discharge/charge cycle of the HPPC test. Once the model is developed, the model is validated by applying it to the entire HPPC data set and measuring the accuracy. Once the model is validated, any power schedule can be put through the model to determine how the cell will perform.

The next step is to use this single-cell model to generate a model that simulates the battery pack performance. The number of cells in the battery pack is calculated based on given specifications of pack voltage and energy. This scaled-up model now can take a power profile and predict the battery pack's performance. This will be discussed in depth in Chapter 4.

2.4 Integration Issues

Intuitively, developing a model that simulates a battery pack's performance should only consist of scaling a single-cell model by the number of cells. However, this method will produce

inaccurate results, due to the fact that when creating a battery pack, cells are not the only component. As discussed in the sections 2.1 and 2.2, a battery pack for an electric vehicle consists of the cells, the cell housing, connectors and bus bars, a battery management system and a thermal management system. Therefore, the total battery pack weight cannot be calculated by scaling the weight of one cell by the total number of cells in the pack. This increase in battery pack weight will reduce the effective energy density and power density of battery pack.

For example, the 2011 Nissan Leaf battery pack is made up of 192 $LiMn_2O_4$ with Graphite cells, each weighing 799 g. The total pack weight is 294 kg. The cells therefore contribute to only approximately 52% of the total pack weight [20]. The 2017 Chevy Bolt battery pack is made up of 288 LG flat "landscape" cells. Each cell weighs 850 g. The total pack weighs 440 kg, resulting in the cells making up 55.63% of the total pack weight.

Another important factor in accurately simulating battery pack performance is the format of the cell being used in the battery pack. Cylindrical and pouch cells are the most popular types of cells for electric vehicles, and each have their own advantages and disadvantages. For example, pouch cells tend to be higher capacity and energy than cylindrical cells, so fewer are required to achieve a certain power/energy specification. Since, pouch cells are larger, they have a large temperature gradient across the layered active material. This will accelerate the thermal aging of the cell, thereby requiring a more sophisticated thermal management system. In order to develop a model that accurately simulates battery pack performance, all of these factors need to be accounted.

Chapter 3: NASA – ULI Cell Selection Methodology

3.1 Introduction

NASA has announced a goal of over 70% fuel burn reduction by 2025. In accordance with this goal, NASA has launched a University Leadership Initiative (ULI) involving several universities collaborating across the United States to create a hybrid electric aircraft that achieves upwards of 20% fuel reduction. These universities consist of Ohio State University (OSU), Case Western Reserve University, Georgia Institute of Technology, University of Wisconsin, University of Maryland and North Carolina State University. The initiative is focused on hybridizing a small, regional aircraft. The hybrid architecture that the team at OSU is researching to implement is a series hybrid that also can work as a series-parallel architecture in some conditions. The series hybrid architecture uses a gas turbine in series with the battery pack, causing the power outputs of each to be added together to provide energy to the motor. On the other hand, a series-parallel hybrid architecture combines the parallel hybrid and turboelectric designs, as discussed in Chapter 1. This architecture combines mechanical energy produced by the gas turbine with the energy from a battery pack to provide electric energy to the motor.

The cell selection process begins with defining a mission profile. The team at Georgia Tech has created several mission profiles that list the continuous power requirement for the given mission. Figure 11 below shows an example of a mission profile developed by Georgia Tech. This mission profile involves the battery pack providing 30% of the total power required for

takeoff and climb and 20% of the total power required for cruise. The mission power profiles are developed by running several optimization algorithms, including dynamic programming and optimal control, to create the most fuel-efficient mission involving both the gas turbine engine and the battery pack. It is important to note that although the mission profile consists of both gas turbine power output and battery pack power output, this analysis will only consider the power required by the battery pack for the energy storage system design.

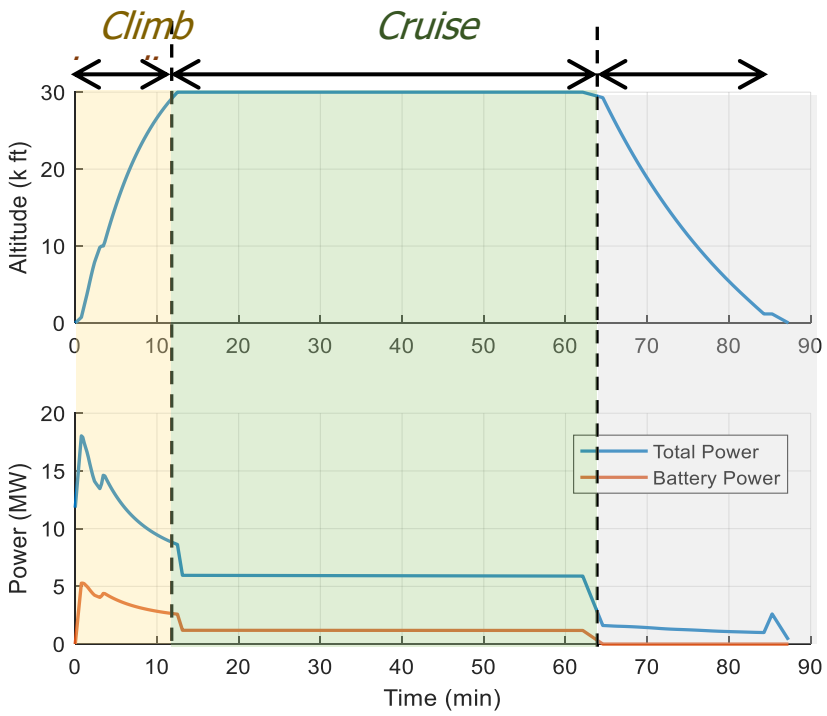

Figure 11: Mission Profile

Along with the mission profile, an important factor in cell selection is the power and energy requirements of the battery pack. For the NASA – ULI project, the battery pack must be designed to produce an instantaneous maximum power output of 8 MW and an energy of 2 MWh. The team selected a maximum voltage of 2 kV for the battery pack. However, during the mission, the pack will not operate at this voltage level due to the characteristics of the cells. The behavior of the pack will be simulated by a model, as will be discussed in Chapter 4.

3.2 Cell Selection Methodology

Selecting the cell technology that will be used to create a battery pack is a complicated process. The process involves several rounds of testing and data analysis, which can require several weeks or months depending on the protocol. However, selecting the proper cell for the battery pack is one of the most important decisions for the optimal performance of the battery pack. Figure 12 below is a flow chart depicting the cell selection process for the NASA – ULI project. The original cells selected (left side of chart) were chosen as best-in-class, commercially available cells based on the datasheets provided by the manufacturers.

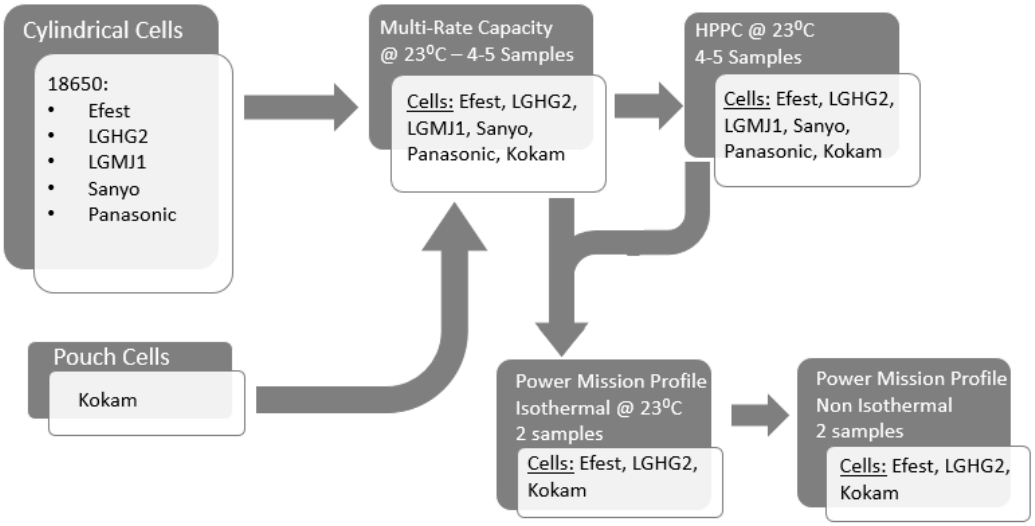

Figure 12: Flow chart of cell selection process

The cell selection process is mainly comprised of running the Multi-Rate Capacity tests on the cells and analyzing the data. HPPC testing on the cells is generally used for model development, but also used to determine how much heat the cell generates during operation. All the cells undergo Multi-Rate Capacity testing and then HPPC testing. The top performing cells are then chosen and tested with the mission profile to determine how it will perform.

A precursor to these steps is deciding which cell technologies will be considered. For this project, the OSU team investigated commercially available as well as advanced cell technologies. As stated at the end of Chapter 1 and in Figure 13 below, commercially available off-the-shelf cell technologies of the present day have energy densities in the range of 170-270 Wh/kg, according to their datasheets. The advanced cell technologies range between 350-500 Wh/kg, however they are prototypes.

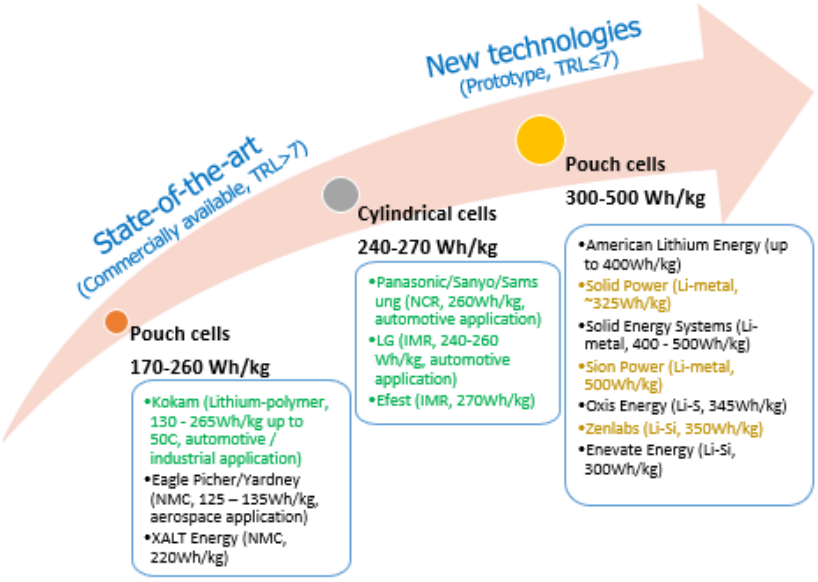

Figure 13: Cell technology of today

3.3 Identification of High Energy Density Cells

The team investigated five state-of-the-art commercially available cylindrical cells, one commercially available state-of-the-art pouch cell, and one advanced technology pouch cells. The five cylindrical cells that were tested are the Efest IMR18650, LG 18650HG2, LG INR18650MJ1, Panasonic NCR18650B, and the Sanyo NCR18650GA. The commercially available pouch cell that was tested is the Kokam SLPB065070180. The advanced technology cell that were considered is the ZenLabs ENV35011CRC. The advanced technology cell analysis

will not be included in this thesis, as testing is still being conducted. The team purchased five samples of each cylindrical cell technology and four samples of the Kokam pouch cell to test the samples and determine sample variation in the technology.

The main stage of testing for the cell selection process consists of running Multi-Rate Capacity tests on the samples. The test was run following the protocol and standards of the USABC Electric Vehicle Test Manual [21]. The specific current discharge rates (C-rates) were C/3, C, 2C, and 10 Amps, where "C" is the rated current that charges the cell to full capacity in one hour. Data from the test was then analyzed and plotted to visualize how the capacity and energy of the cells change as the cell is discharged at different C-rates. Figure 14 below is a plot of the Efest IMR cell Multi-Rate Capacity test results. The figure shows how the Efest cell has low variability in its capacity at higher C-rates. Figure 15 below is a plot of the LG MJ1 cell Multi-Rate Capacity test results. The figure shows that at higher C-rates, the LG MJ1 cell has large variability in its capacity. Figures 16 and 17 show the energy of the cell at different rates. These plots depict the same results; the Efest cell is more stable at higher C-rates, while the LG MJ1 loses a lot of energy at higher C-rates. Maintaining optimal capacity at higher C-rates is crucial for aerospace application, as the HEA will often require high current outputs. Therefore, this metric of maintaining close-to-optimal capacity and energy at higher C-rates was used in this project to eliminate cell technologies during the cell selection process.

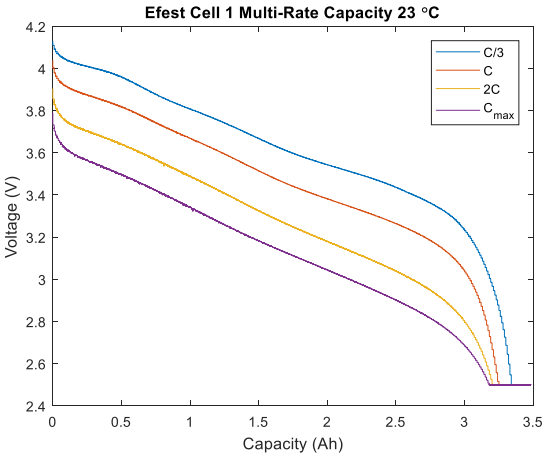

Figure 14: Efest capacity vs. C-rate

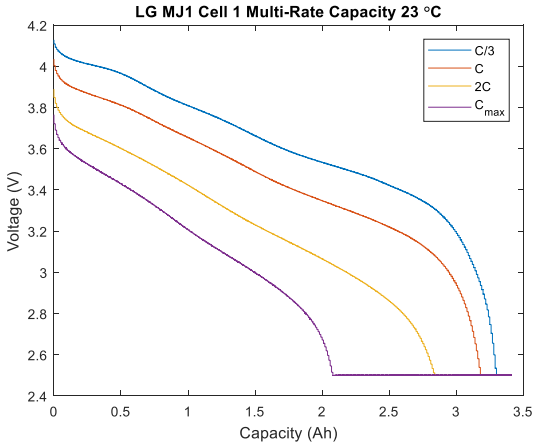

Figure 15: LG MJ1 capacity vs. C-rate

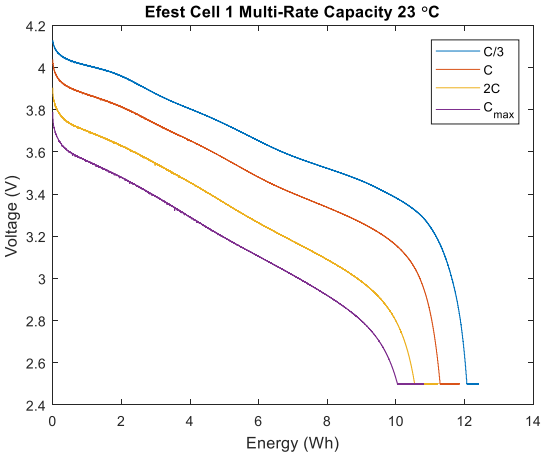

Figure 16: Efest energy vs. C-rate

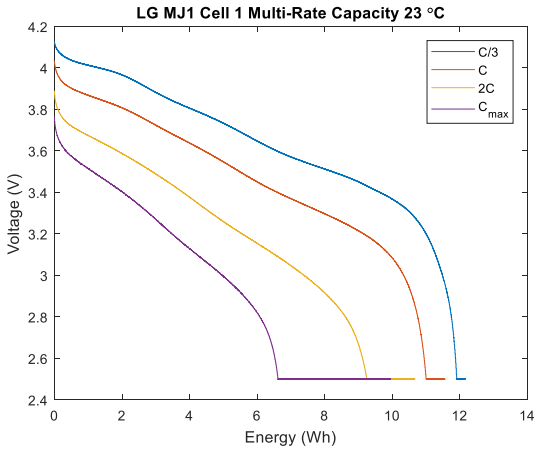

Figure 17: LG MJ1 energy vs. C-rate

The team used the decrease of capacity at higher C-rates as a metric to decide whether or not a cell would continue on to the next stage of testing for the project. The LG MJ1 and Panasonic cells had large degradation of capacity at high C-rates. Therefore, the NASA – ULI project eliminated these two technologies options. However, the team decided to continue testing all the samples for these technologies for research purposes.

Multi-Rate capacity tests were run on all the cell samples to determine the sample variation of capacity and energy density of the technologies. The data from the Multi-Rate

capacity tests were used to determine the energy density of each sample. The cell energy when the cell initially reaches its minimum voltage was recorded. The minimum cell voltage for all technologies investigated in this thesis is 2.5 V. The energy density (Wh/kg) of the sample is calculated by dividing the energy (Wh) recorded at V_{min} by the sample weight (kg). V_{min} is the minimum voltage of the cell recommended by the manufacturer. Figure 18 below depicts a plot comparing all the different technologies' energy density and the sample variation. The errorbar function in MATLAB was used to plot the deviations of the samples per cell technology.

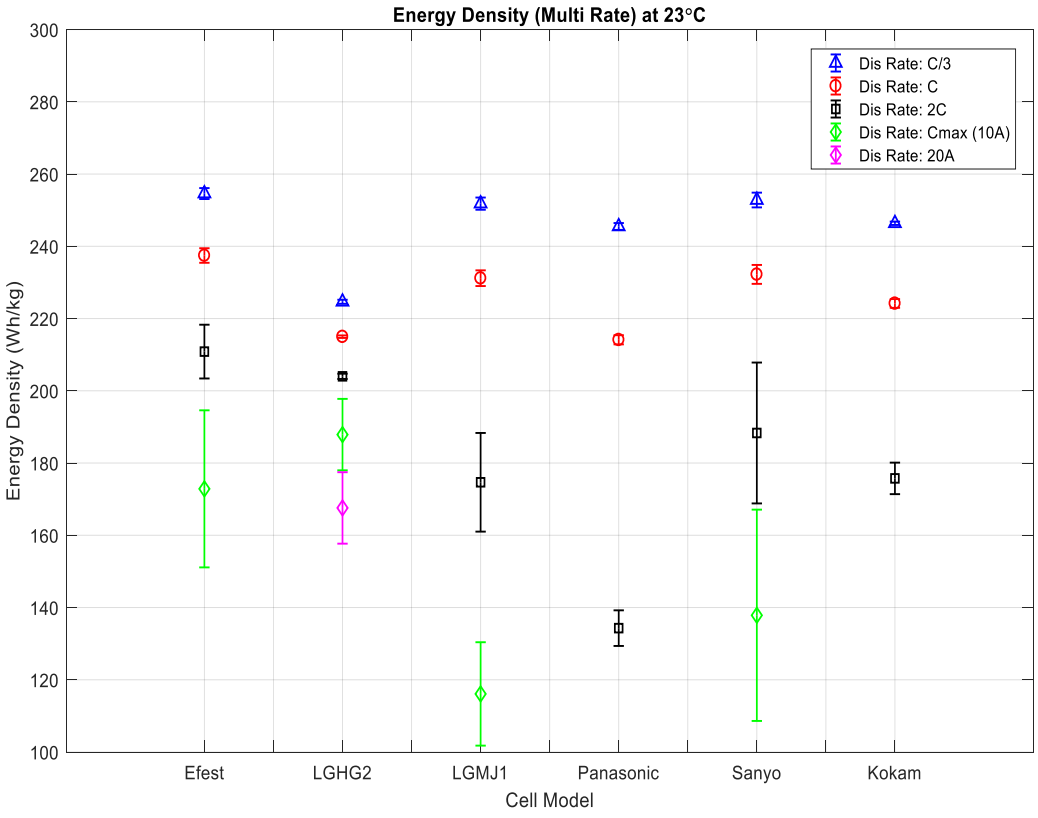

Figure 18: Energy density comparison

The team used sample variation as another metric to decide whether a cell would continue on to the next stage of testing. The Sanyo cells have very high variation in energy

density at higher C-rates. Therefore, the project eliminated the Sanyo cell technology as an option. The LG HG2 and Kokam cells all have very low variability at higher C-rates. Based on the data collected and the conclusions made above, the team decided that the Efest, LG HG2, and Kokam cells are the most promising cells regarding the energy density.

An interesting conclusion was made when running the Multi-Rate Capacity tests on the cells. For most cell technologies, the datasheet provided by the manufacturer depicted a higher energy density and capacity than was experimentally determined. For example, the LG HG2 data sheet [22] states the cell has an energy density of 240 Wh/kg at C/5. However, after experimental testing, the team found the energy density to be 224 Wh/kg at C/3. Although the energy density from the datasheet was determined using a C/5 discharge, the trend in the data does not attest that the energy density would increase to 240 Wh/kg by decreasing the C-rate to C/5. Figure 18 uses a linear extrapolation to approximate the value of the energy density of the LG HG2 cell at C/5. According to Figure 19, the energy density could be approximated to be 240 Wh/kg. However, when a parabolic extrapolation is used to approximate the C/5 energy density of the cell, it is apparent by visual inspection that the energy density cannot be approximated be 240 Wh/kg. Rather, it should be approximated to 230 Wh/kg, as shown in Figure 20 below. The parabolic extrapolation fits the data more accurately, therefore the parabolic approximation should be used when estimating the energy density of the LG HG2 cell.

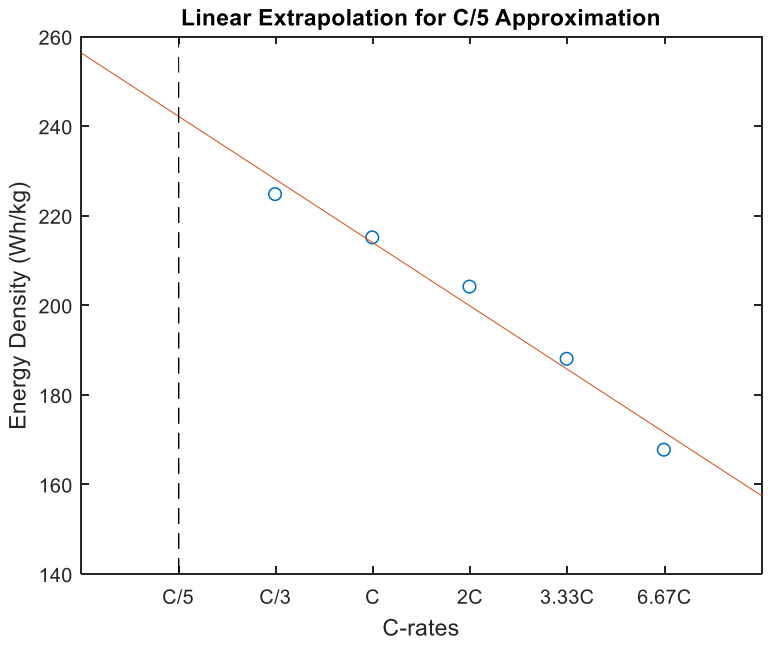

Figure 19: Linear approximation of C/5 energy density of LG HG2

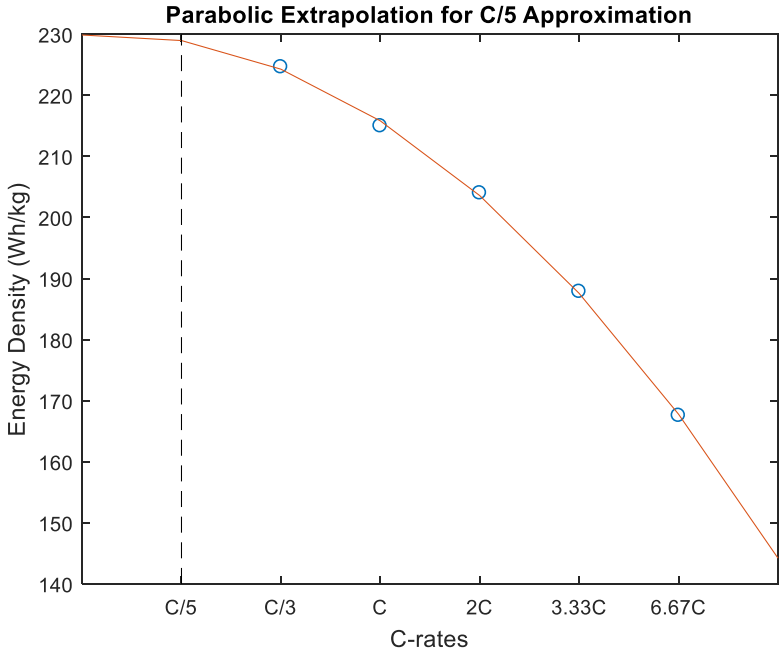

Figure 20: Parabolic approximation of C/5 energy density of LG HG2

The datasheet also stated that the nominal capacity of the LG HG2 cell is 3.0 Ah. However, this capacity is only achievable at a discharge rate of C/5. A plot of the experimental results of the Multi-Rate Capacity test for the LG HG2 cell is shown below in Figure 21. The

figure shows that when discharging the cell at C, the LG HG2 cell has a capacity closer to 2.8 Ah. Although this difference may not seem too important, it will have major implications on the battery pack design.

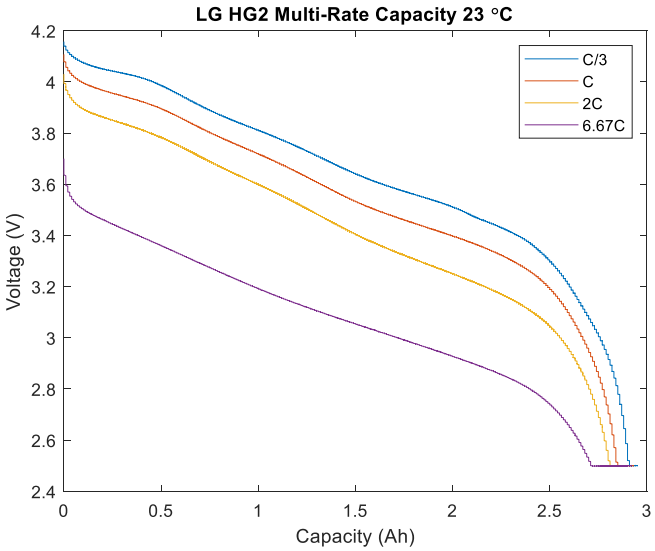

Figure 21: LG HG2 capacity vs. C-rate

The data acquired from the Multi-Rate Capacity tests about the cell technology and the trend that the cell's capacity and energy density degrade as the C-rate increase is crucial to understand when designing the battery pack. If a battery pack is designed using the capacity and energy density information provided in the data sheet, the pack may be undersized. Due to the lack of standardization, the capacity and energy density information from the data sheet is measured at a very low discharge rate, such as C/10. In normal operation, cells in battery pack are discharging at rates such as C or higher when necessary. From the trend that is explicitly shown in Figures 13 – 16, the capacity and energy density of a cell decreases as the discharge rate increases. Therefore, if a pack is sized using the capacity and energy density provided by the data sheet, the pack may not meet the specifications under normal operation. This test data is crucial for battery pack design as it provides information about the cell's capacity and energy

density at higher C-rates and allows the pack to be designed to meet the specifications under normal operation.

3.4 HPPC Testing

The next step after the Multi-Rate Capacity test is to determine the internal pulse resistance and the power capabilities of the cell. The internal resistance is the resistance of a cell due to the resistivity of the cathode and anode and imperfections in the process of ion transfer between the cathode and anode.

Internal resistance was used as another criterion for deciding which cells to continue testing. If the cell has a high internal resistance, it will generate more heat during operation. More heat can cause the cell to degrade more quickly if not properly managed, thereby requiring a more sophisticated and expensive thermal management system. Therefore, a cell with high internal resistance was deemed less suitable for the project.

Determining internal resistance is done using a dynamic test. For the NASA ULI project, the HPPC (Hybrid Pulse Power Characterization) test was used. The HPPC test run on the cells also followed the USABC protocol and was run at isothermal temperature (23 °C) and atmospheric pressure (101.325 kPa). The HPPC tests consists of a series of charging and discharging stages that are calculated to decrease the state of charge (SOC) of the cell by a specified amount. A decrease of 10% SOC was used for the HPPC testing in the NASA – ULI. Data from the test was then analyzed, and the internal resistance was calculated for each cell sample at each 10% increment in the SOC.

The process of calculating internal resistance depends solely on the HPPC data. A portion of each stage of the HPPC test involves allowing the cell to rest for one hour. The value at the end of the resting period is considered to be the open-circuit voltage (OCV) of the cell at that SOC. The cell is then discharged for 30 seconds at 1C, then allowed to rest for 40 seconds, and finally recharged for 10 seconds. The cell is then discharged at a current rate of C/3 until it reached an SOC level of 10% lower than the previous pulse. The cell rests for one hour before the next pulse occurs. This process occurs 10 times, discharging the cell from 100% SOC to 0% SOC. Based on this data, internal resistance is calculated at each 10% SOC interval by the following equation:

$$R(SOC) = |V_{start}(SOC) - V_{end}(SOC)|/|I_{end}(SOC) - I_{start}(SOC)| \quad (1)$$

$V_{start}(SOC)$ is the voltage of the cell at the beginning of the charge or discharge portion of the pulse. $V_{end}(SOC)$ is the voltage at the end of the discharge/charge portion. Similarly, $I_{start}(SOC)$ and $I_{end}(SOC)$ are the currents at the beginning and end of the charge or discharge portions. Figure 22 below plots the voltage and current during the HPPC test.

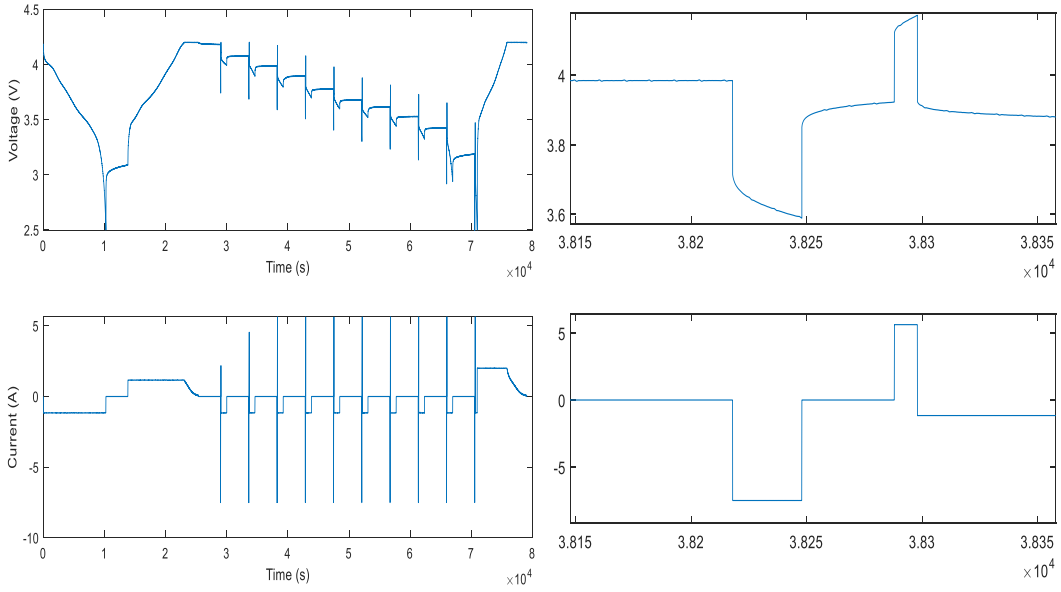

Figure 22: Voltage and current from HPPC test

It is important to note that since V_{start}, V_{end} , I_{start} , and I_{end} have different values for charge and discharge. Therefore, the internal resistance will have different values for the charge and discharge portions at each SOC interval. This is due to the electrochemistry of the cell and how the materials inside the cell react differently to charging and discharging. The internal resistance was calculated at each 10% SOC interval.

Figure 23 below plots the internal resistance values for an Efest cell. The graph plots the internal resistance at each 10% interval of SOC, and includes an errorbar to show the variation between the five different samples for Efest. From visual inspection, the variation between samples for Efest is very low. Low variation in internal resistance was also found to occur in the other cell technologies.

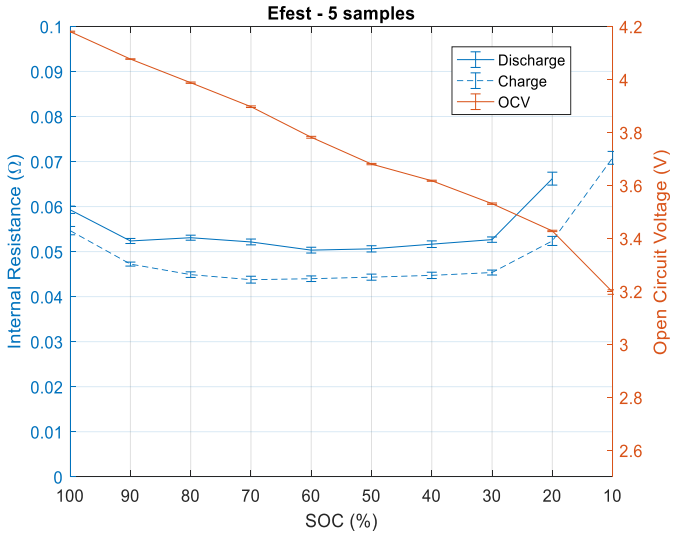

Figure 23: Efest internal resistance

Not only is the HPPC data used to calculate internal resistance of the cell, it can also be used to calculate the maximum output power capacity of the cell at each 10% SOC interval. Specifically, the internal resistance and the OCV are used to calculate the maximum power provided by the cell at each SOC interval. The power is calculated using the following equation:

$$Power_{maximum}(SOC) = V_{minimum} * (\ OCV(SOC) - V_{minimum})/R(SOC) \qquad (2)$$

$V_{minimum}$ is the minimum voltage of the cell, which is provided by the manufacturer. The cells tested for the NASA – ULI have a minimum voltage of 2.5 V and a maximum charge voltage of 4.2 V. The OCV is the voltage of the cell at the end of the hour-long rest period at each 10% SOC interval, as discussed above. Similar to the internal resistance, the maximum power for charge and discharge of the cell can be calculated depending on whether the charge or discharge resistance value is used. To calculate the maximum charge power of the cell, the charge internal resistance must be used in the equation. For maximum discharge power, the discharge internal resistance must be used in the equation. Figure 24 below is a plot of the maximum discharge and charge power for the Efest cells. The errorbar function was used to show the variation between the five different samples. From visual inspection, the variation between samples is very low. Low variation in maximum power was found to occur in the other cell technologies as well.

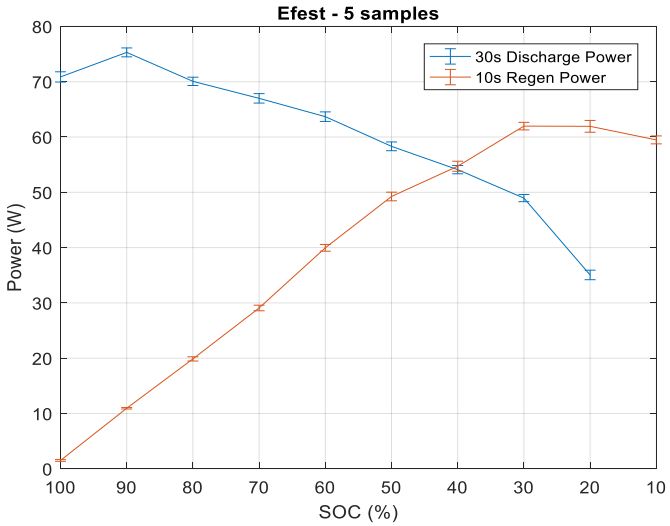

Figure 24: Efest maximum output power

All cylindrical cells tested were found to have very similar internal resistance values (40-60 mΩ). Therefore, the internal resistance of cells was not a factor in determining which cells would continue to be tested. Nevertheless, the LG HG2 was found to have the lowest internal

resistance of all cylindrical cells at <40 mΩ. This allows the cell to have a maximum charge and discharge power significantly higher than all other cells except Kokam. Figure 25 plots the maximum power of the LG HG2 cells, providing a max discharge power of over 110 W at 100% SOC.

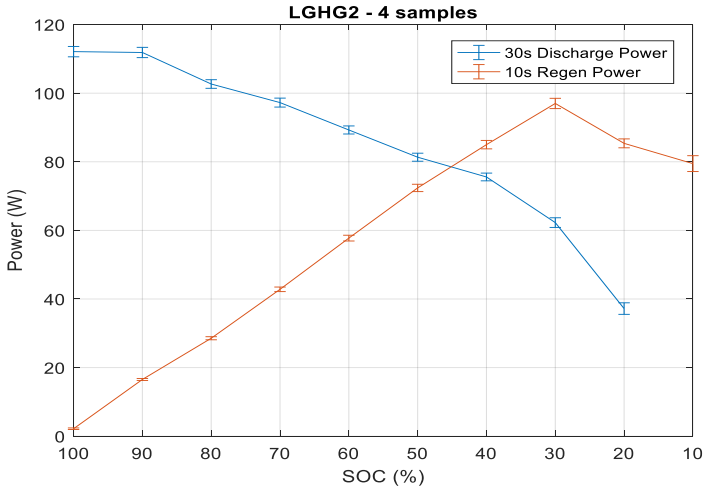

Figure 25: LG HG2 maximum output power

Another interesting finding was made regarding the Kokam cells. The internal resistance of the Kokam cells is ~10 mΩ as seen in Figure 26, significantly lower than the other cell technologies. Since the Kokam cell is a pouch cell, which have larger surface areas than cylindrical cells, this allows the ions to have more paths available to travel, thus decreasing the amount of collisions between ions. Additionally, the cathodes and anodes are placed near each other, reducing the distance the ions travel.

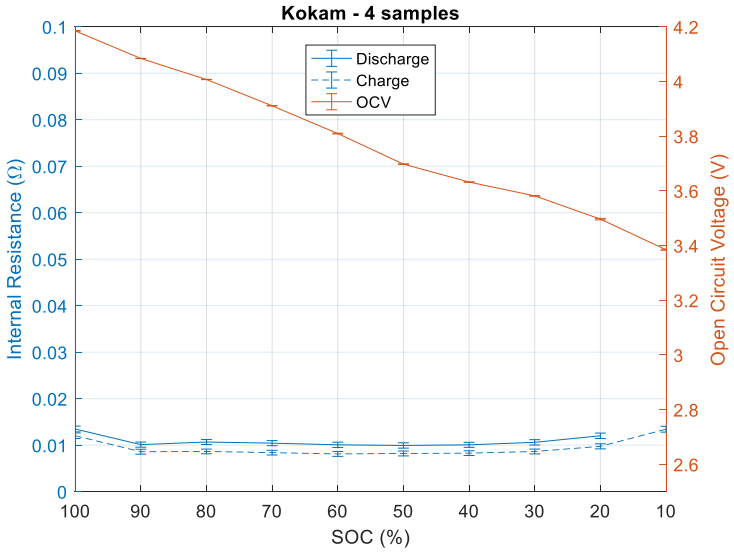

Figure 26: Kokam internal resistance

Not only does Kokam have the lowest internal resistance, it can support the largest discharge current of 24 A due to its larger size. The combination of the extremely low internal resistance and high discharge current allow the Kokam to provide the largest maximum charge and discharge. Figure 27 below plots the charge and discharge power for Kokam. The cell can provide over 400 W at 90% SOC. Notice that the cell variation in max power is larger than the other cells.

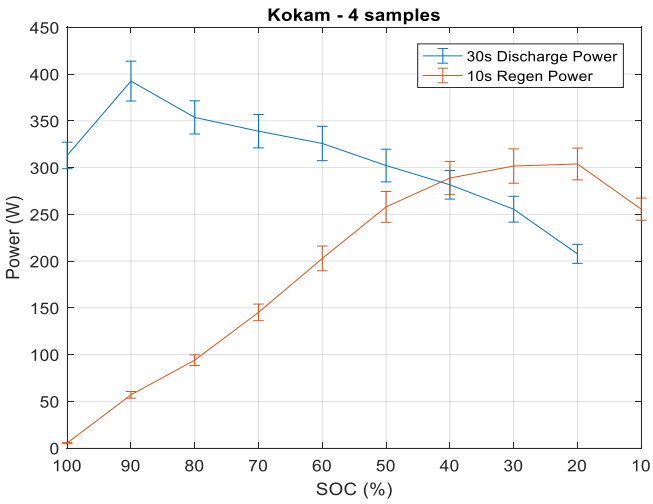

Figure 27: Kokam maximum output power

Chapter 4: Model Development and Pack Design

Once the internal resistance of the cells was calculated, the next step was to develop a model that simulates the cell's performance for a given power schedule. For scope of this research project, the equivalent circuit model approach has been chosen. Using an equivalent circuit model, the performance of the battery is simulated using an ideal voltage source and a series of resistors and capacitors, depending on what order model is being built. Both 0^{th} and 1^{st} order equivalent circuit models were developed. The 0^{th} order model was developed to be used for battery pack design. The 1^{st} order model will support the project in the future for controls and diagnostics.

4.1 0^{th} Order Model Development

As discussed in Chapter 2, a 0^{th} order equivalent circuit model characterizes the cell's performance using an ideal voltage source (the OCV) and a series resistance (the internal resistance of the cell). The OCV and internal resistance were previously calculated during the HPPC data analysis phase at each 10% SOC interval. However, when developing the model, the OCV and internal resistance are required at every time interval of the power profile. For the NASA – ULI project, the profile is specified at every second. Therefore, the OCV and internal resistance are interpolated using MATLAB's interp1 function to calculate the values at every second.

The power, current, voltage and heat outputs of the cell, along with the SOC of the cell, are required to be calculated at every second as well. The power of the cell at every second is found by interpolating the maximum power output of the cell at every 10% SOC interval

calculated during the HPPC data analysis stage. The power, OCV, and resistance of the cell at every second are used to calculate the current, voltage, heat output, and SOC of the cell with the following equations:

$$I(t) = \eta * \frac{\left(OCV(t) - \sqrt{OCV(t)^2 - 4 * R(t) * P(t)}\right)}{2 * R(t)} \quad (3)$$

$$V(t) = OCV(t) - R(t) * I(t) \quad (4)$$

$$Q(t) = R(t) * I(t)^2 \quad (5)$$

$$SOC(t+1) = SOC(t) - \left(\frac{\left(I(t) * \left((t+1) - t\right)\right)}{3600 * C_{nom}}\right) \quad (6)$$

C_{nom} is the nominal capacity of the cell. The value of C_{nom} is given by the manufacturer is the datasheet. The equation for SOC is unique in that it calculates the SOC of the next second. This is done to account for any limits set on the SOC range of the cell. The initial SOC value is set, allowing the following SOC value to be calculated using the given equation. The limiting of the SOC range will be further explored later in this chapter.

An important note to make is that since the HPPC test data incorporates charge and discharge currents, the values of the current are positive and negative to capture the charge and discharge currents of the HPPC test. Therefore, Equation 3 could possibly output imaginary numbers for the current. In order to account for these imaginary current values, the following equation is used:

$$I(t) = (conj\left(I(t)\right) + I(t))/2 \quad (7)$$

Conj() is the MATLAB function used to calculate the conjugate of an imaginary number. This equation will correct for any imaginary current values calculated using Equation 3.

4.2 0^{th} Order Model Validation

Once the 0^{th} order cell model had been developed, the model required validation. To do so, the model was put through the power schedules provided by Georgia Tech. The cell model was put through the power schedules in order to test the accuracy of the results generated by the model. Figure 28 below plots the simulated and experimental results of the Efest and LG HG2 cells when simulated with the power profile. The specific power profile used in the simulation was 30% Climb - 20% Cruise. This means the battery pack is required to provide 30% of the overall power required during takeoff and climb and 20% of the power during cruise. Figure 28 plots the pack voltage and current of the two cells, since the model was scaled up to simulate pack performance. From visual inspection, the model accurately simulates the cells' true performance when subjected to the power schedule. The model captures the dynamics of the cell very accurately. Consequently, the model can be relied upon to determine whether or not a battery pack can provide the power required for a certain power schedule.

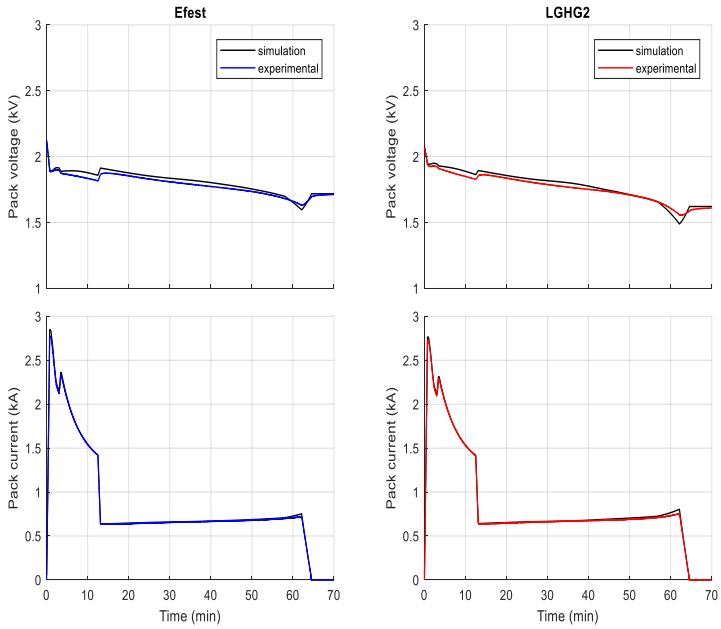

Figure 28: Efest and LG HG2 model validation

Scaling up the model is accomplished by multiplying the results of the simulation in terms of cell voltage and current by the number of cells in series and parallel, respectively. Multiplying the model by the number of cells in series produces the voltage performance of the battery pack. Multiplying the model by the number of chains in parallel produces the current performance of the battery pack. Calculating the number of cells in series and parallel will be discussed later in this chapter.

4.3 1st Order Model Development

Developing a first order model is slightly different than a 0th order model. Since the 1st order model is meant to more accurately represent the dynamics of a cell, the model incorporates two new parameters, R_1 and C_1, as shown in Figure 10. The 1st order model incorporates 4 main parameters: E_0, R_0, R_1, and C_1. The following equations are used to calculate the parameters:

$$E_0(SOC) = OCV(SOC) \quad (8)$$

$$R_0(SOC) = R_{instant}(SOC) \quad (9)$$

$$R_1(SOC) = R_{pulse}(SOC) - R_0(SOC) \quad (10)$$

$$\tau(SOC) = -\log(1 - 0.6321 * R_1(SOC) * |I(SOC + 1) - I(SOC)|) \text{ [23]} \quad (11)$$

$$C_1(SOC) = \tau(SOC)/R_1(SOC) \quad (12)$$

$R_{instant}$ is calculated using Equation 1. However, V_{end} and I_{end} are the voltage and current values at the point immediately after the discharge or charge begins. R_{pulse} is also calculated using Equation 1, with V_{end} and I_{end} being the voltage and current values at the end of the discharge or charge pulses. The OCV is approximated to be the voltage value immediately before the discharge pulse occurs, after the hour-long rest period.

The equation for the time constant is derived by Gregory Plett in his book titled "Battery Management Systems Volume 1, Battery Modeling". The time constant τ incorporates the capacitive discharge of the cell. As shown in Figure 21, the cell's voltage drops very quickly, then declines in a manner similar to a capacitor losing voltage.

It is important to note that equations 8 – 12 provide an initial estimate to the value of these parameters. An optimization algorithm must be run in order to minimize the error between the experimental data and the simulated data. For this project, the fminsearch function in MATLAB was used to perform the optimization. Once these parameters are optimized, the model can be used to simulate the cell's performance. However, using fminsearch can be time consuming to perform every time the model is needed to simulate the cell's performance. For this reason, it is not used for battery pack design. 1^{st} order models are more typically used in control and diagnostics of the battery pack.

The 1^{st} order model was calibrated using the HPPC test data at each 10% SOC interval. Figure 29 below plots the HPPC test data and the simulated results for the 80% SOC region discharge pulse. The model accurately captures the dynamics of the cell's discharge pulse, achieving an RMS error of 2.8 mV for this discharge pulse. The RMS error throughout the 10% SOC intervals are all within the 0.1 – 3 mV range, showcasing the accuracy of the 1^{st} order model.

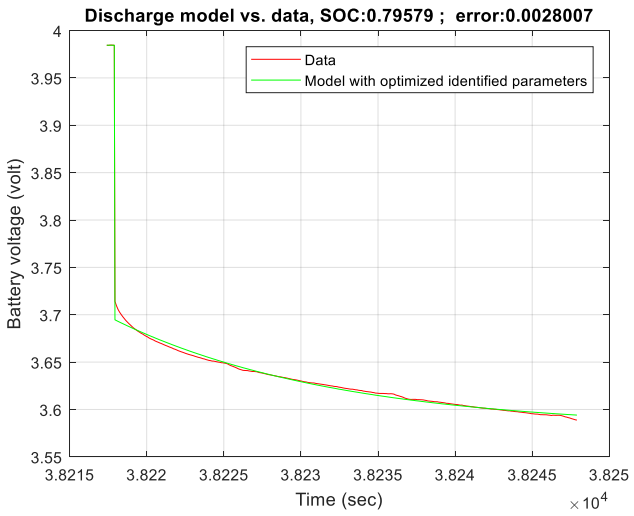

Figure 29: 1st order mode calibration

4.4 1st Order Model Validation

Once the 1st order model had been developed and calibrated for every 10% SOC interval, the next step was to validate the model over the entire HPPC test data, beginning from the first discharge pulse at 100% SOC and ending at the 0% SOC interval. Figure 30 below plots the 1st order model data and the experimental data of the HPPC test. The model captures the capacitive dynamics of the cell during discharge and charge. However, the model does not capture the dynamics of the cell during the resting period.

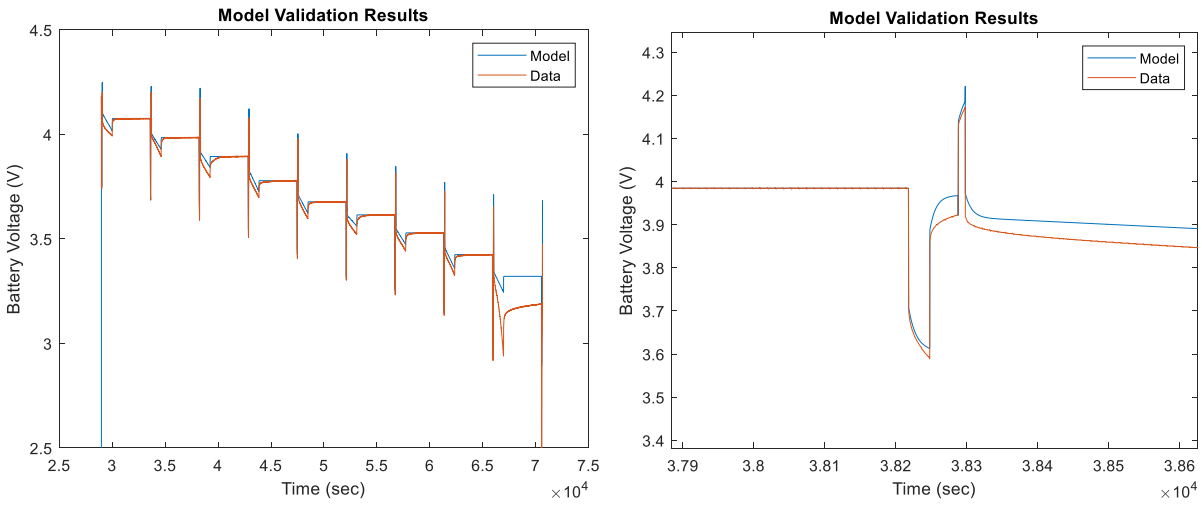

Figure 30: 1st order model validation - HPPC test data

The RMS error was calculated between the model and experimental results. The error was calculated to be 24.7 mV. Figure 31 below plots the error at every point between the model and the experimental data. Figure 31 depicts that the error is very high during the portion when the cell is being discharged to 10% SOC lower than the previous SOC value. The lowest error occurs during the during the 10% SOC discharge portion and the hour-long rest period.

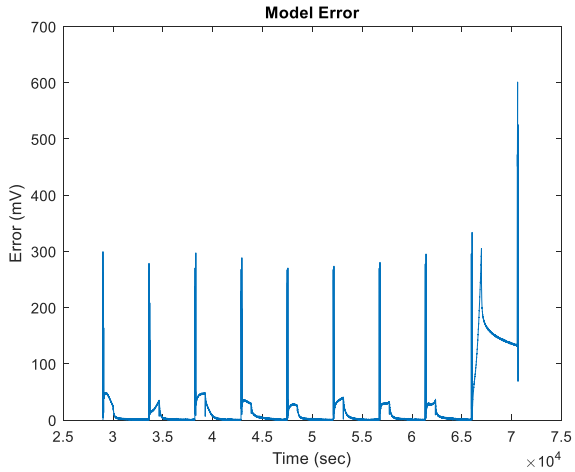

Figure 31: 1st order model error

The figure also shows that the error is the largest at the last 10% SOC interval. This is due to the electrochemistry of the cell and the fact that the cell has gone through a minor aging process throughout the course of the test, slightly deteriorating the cell and decreasing its

performance during the final pulse. Excluding the final 10% SOC interval, the RMS error was calculated to be 11.8 mV.

Additionally, the 1st order model was validated using the power schedule data, as pictured in Figure 11. Figure 32 below shows the results of this validation. Again, the model accurately captures the dynamics of the cell during discharge. However, throughout the plot, there is a slight offset between the model and the data.

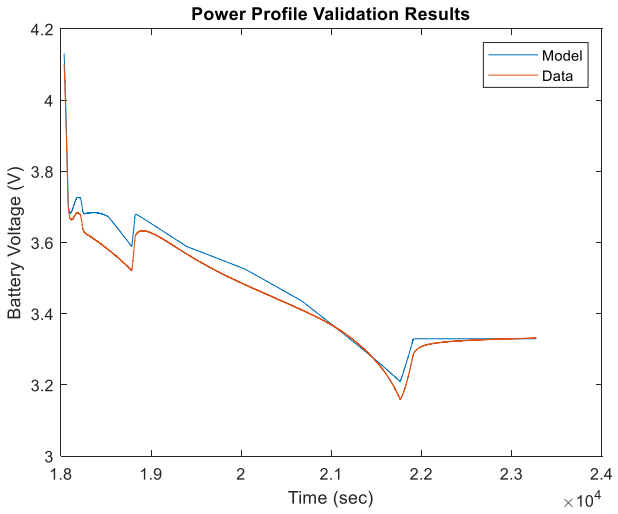

Figure 32: 1st order model validation - power profile

The RMS error for this validation was calculated to be 26.4 mV. Figure 33 below plots the error at every point between the model and the experimental data. The figure shows the largest error occurs during the initial discharge pulse of the power schedule.

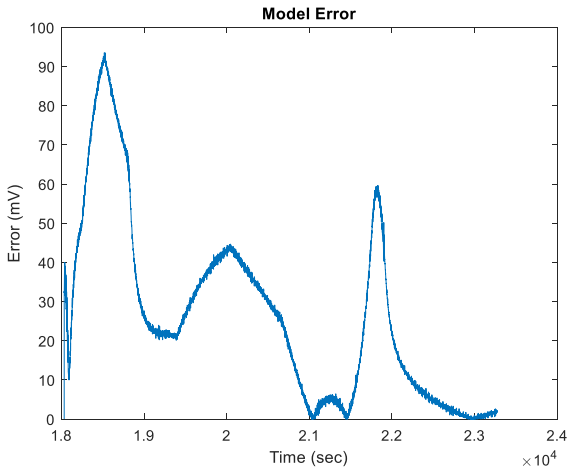

Figure 33: 1st order model error

4.5 Preliminary Pack Design

Designing a pack is mainly comprised of connecting the cells in a way that produces a specified pack power or energy. These specifications are generally given to the designer. The two ways to connect the cells in a battery pack are series and parallel connections. Cells are connected in series to achieve a specified pack voltage. These series chains are connected in parallel to achieve a pack current and energy. The following equations are used to calculate the number of cells in series and parallel:

$$N_{cell} = \frac{E_{batt} * 1000}{V_{nom} * C_{test}} \quad (13)$$

$$N_{series} = \frac{V_{max,\ pack}}{V_{max,\ cell}} \quad (14)$$

$$N_{parallel} = \frac{N_{cell}}{N_{series}} \quad (15)$$

E_{batt} is the required energy of the battery pack. This parameter is calculated by calculating the area under the power requirement curve. V_{nom} is the nominal operating voltage for the cell technology being simulated. This value is provided by the manufacturer in the datasheet. C_{test} is

the capacity of the cell at 1C found during experimental testing. $V_{max,pack}$ is the maximum operational voltage of the pack. For this project, the maximum pack voltage was 2000 V. $V_{max,cell}$ is the maximum voltage of the cell. Since this project only investigated Li-ion cells, this value was 4.2 V for all cell technologies.

Using these variables, the 0^{th} order cell model can be scaled up to simulate pack performance. In order to simulate the pack's voltage during the power profile, the cell model voltage results are simply multiplied by N_{series}. To simulate the pack's current output during the power profile, the cell model's current results are simply multiplied by $N_{parallel}$. This method was used to generate the results pictured in Figure 28 during the 0^{th} order model validation.

This process is very powerful, as it allows a designer to simply simulate a battery pack's performance for a given power schedule. Using this method, the battery pack responses of the Efest, LG HG2, and Kokam cells were simulated for the power schedules provided by Georgia Tech. Figure 34 below plots the altitude of flight, the required battery pack output power, and the SOC of the pack over the given profile. The specific profile plotted is 30% Climb – 20% Cruise.

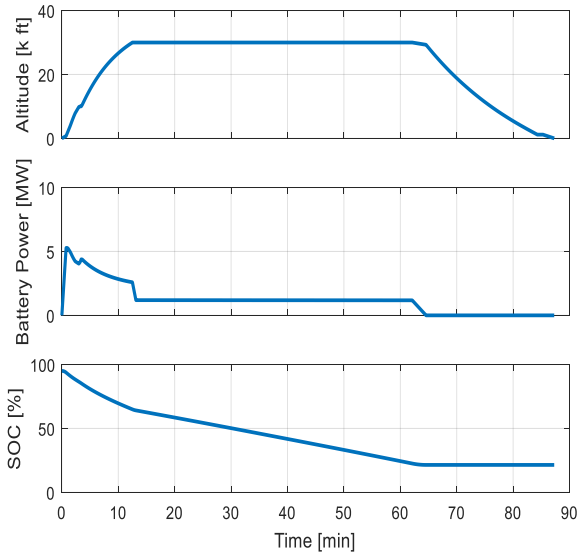

Figure 34: Power profile

The cell models were scaled up using the variables in Equations 13 – 15. Figure 35 below plots the simulated performance of the battery packs consisting of each type of cell. The figure shows that at maximum power output, the battery packs of all three cell technologies surpass the required power output of the profile. Figure 35 also plots the pack C-rate, which are all identical since the same power profile is used for each pack simulation. The pack efficiency is plotted, showing how the pack efficiency is lowest during takeoff and climb. This is expected, since the largest current output is required during this period.

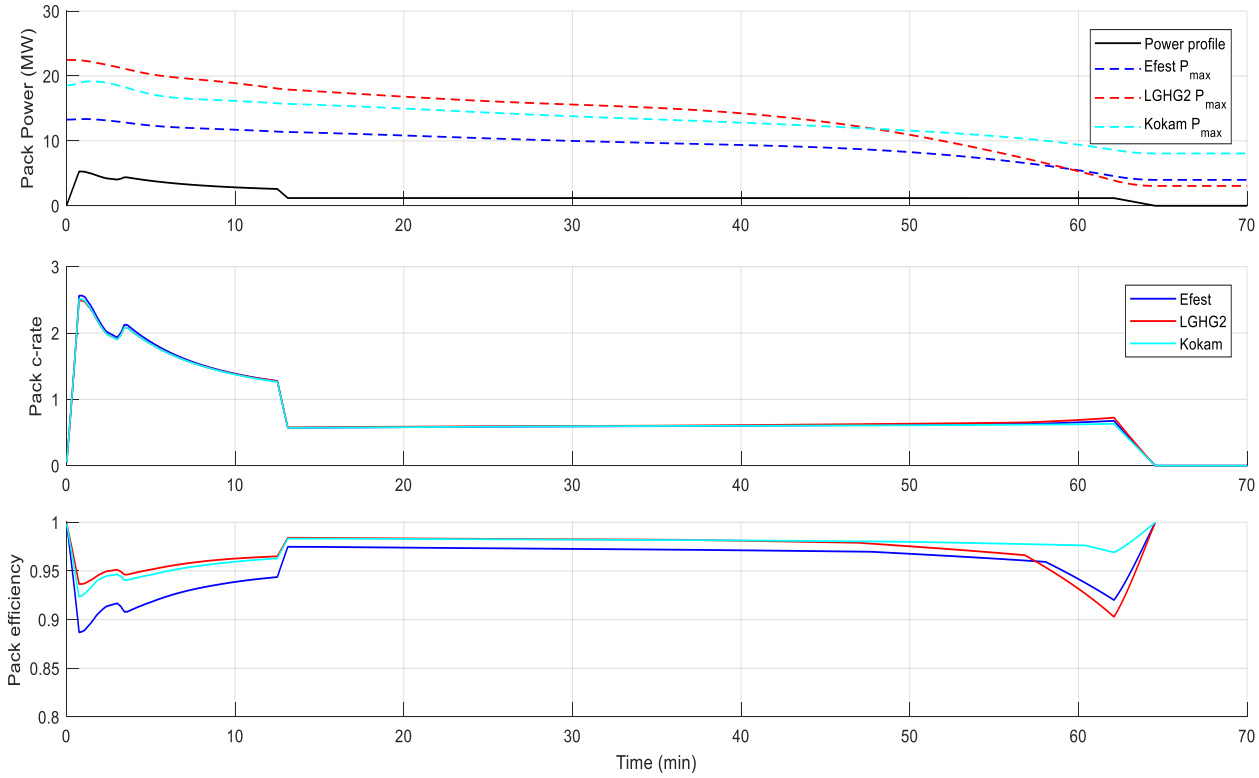

Figure 35: Pack performance for given power profile

This ability to simulate the battery pack's performance for a given power schedule is a very powerful tool. It allows for quick and accurate results when questioning whether or not a cell technology will be able to provide enough power for a given profile. This method is very time efficient and cost efficient, as a battery pack prototype for each cell technology is not required to test whether or not the pack can provide the required power for a mission.

Chapter 5: Future Work

The HPPC test was run at isothermal temperature and atmospheric pressure. Therefore, the 0th and 1st order models developed from the HPPC data are only valid under these conditions. The next step is to expand the model to incorporate the cell response at non-isothermal temperature and non-atmospheric pressures. Specifically, since the model is being used for aerospace application, the model will incorporate cell response at up to ¼ atmospheric pressure (~25 kPa), which is the air pressure at cruising altitude for aircraft.

References

[1] IATA, “Economic performance of the airline industry.” Jun-2018

[2] Datta, Koushik. “UNIVERSITY LEADERSHIP INITIATIVE (ULI) - 2017.” NASA, NASA, 2017, nari.arc.nasa.gov/uli2017#ULI2017List

[4] Lin, C., Mang, J., Grizzle, J.W. and Peng, H. (2001), “Energy management for a parallel hybrid electric truck”, Proceedings of American Control Conference, Arlington, VA

[4] Georgia Tech, Trawick Thesis

[5] https://www.grc.nasa.gov/vine/wp-content/uploads/sites/91/Rodger-Dyson-NASA-Hybrid-Electric-Aircraft-Propulsion-10-4-2017-FULL.pdf

[6] NASA, *Advanced Concept Studies for Subsonic and Supersonic Commercial Transports Entering Service in the 2030-2035 Period*, in *NASA Research Announcement, Pre-Proposal Conference*. 2007, National Aeronautics and Space Adminstration.

[7] Jankovsky, A.L. Overview of Advanced Air Transport Technololgy (AATT) and Hybrid Gas-Electric Propulsion (HGEP). in HGEP NRA Review Meeting. 2017. Cleveland, Ohio

[8] Janson, Ralph. “Overview of NASA Electrified Aircraft Propulsion Activities.” Https://Ntrs.nasa.gov/Archive/Nasa/Casi.ntrs.nasa.gov/20180000593.Pdf, 16 May 2017.

[9] Perry, Dominic. “EasyJet Unveils Short-Haul Electric Aircraft Ambition.” *Flightglobal.com*, 27 Sept. 2017, www.flightglobal.com/news/articles/easyjet-unveils-short-haul-electric-aircraft-ambitio-441543.

[10] Sanford, Jill. *Electric Cars and the Future of Transportation*. 25 June 2018, protectourwinters.org/electric-vehicles-and-the-future-of-transportation/.

[11] “How Much Fuel Does an International Plane Use for a Trip?” Edited by HowStuffWorks, HowStuffWorks Science, 28 Jan. 2015, science.howstuffworks.com/transport/flight/modern/question192.htm.

[12] Schlachter, Fred. “The Back Page.” American Physical Society, Aug. 2012, www.aps.org/publications/apsnews/201208/backpage.cfm.

[13] Hawkins, Andrew J. “Electric Flight Is Coming, but the Batteries Aren't Ready.” The Verge, The Verge, 14 Aug. 2018, www.theverge.com/2018/8/14/17686706/electric-airplane-flying-car-battery-weight-green-energy-travel.

[14] Panda, Sanjib. “Ragone-Plot-Energy-Storage.” ResearchGate, Dec. 2010, www.researchgate.net/figure/Ragone-plot-for-comparing-the-energy-storage-technologies-and-their-power-density-versus_fig6_221909845.

[15] Department of Energy, U.S. “U.S. Battery Storage Market Trends.” U.S. Energy Information Administration, May 2018, www.eia.gov/analysis/studies/electricity/batterystorage/pdf/battery_storage.pdf.

[16] Hughes, Jason. “Pics/Info: Inside the Battery Pack.” Tesla Motors Club, 20 Aug. 2014, teslamotorsclub.com/tmc/threads/pics-info-inside-the-battery-pack.34934/.

[17] Module, ME. “BMS Battery Management System for 12V.” Carousell, 2018, sg.carousell.com/p/bms-battery-management-system-for-12v-116005305/.

[18] Maughan, Ryan. “What Is the Best Electric Vehicle Battery Cooling System?” AVID Technology, 1 Nov. 2018, avidtp.com/what-is-the-best-cooling-system-for-electric-vehicle-battery-packs/.

[19] Glaser, Oli. “How to Measure Capacity of a Lithium-Ion Battery.” Electrical Engineering Stack Exchange, 25 Aug. 2011, electronics.stackexchange.com/questions/18612/how-to-measure-capacity-of-a-lithium-ion-battery.

[20] Gray, Tyler, et al. “2011 Nissan Leaf VIN 0356 Electric Vehicle Battery Te St Results.” Https://Avt.inl.gov/Sites/Default/Files/Pdf/Fsev/batteryrpt2011NissanLeaf0356.Pdf, Dec. 2016.

[21] https://www.uscar.org/guest/article_view.php?articles_id=74

[22] Co., Addicore. “LG INR 18650 HG2 (INR18650HG2) Lithium-Ion Batteries with Case.” Www.addicore.com, 2014, www.addicore.com/HG2-18650-Batteries-p/ad309.htm.

[23] Plett, Gregory L. Battery Management Systems. Vol. 1. Boston: Artech House, 2016. Print.